

South Dakota State University
**Open PRAIRIE: Open Public Research Access Institutional
Repository and Information Exchange**

GSCE Faculty Publications

Geospatial Sciences Center of Excellence (GSCE)

6-18-2018

Large Scale Climate Oscillation Impacts on Temperature, Precipitation and Land Surface Phenology in Central Asia

Kirsten M. de Beurs

University of Oklahoma, kdebeurs@ou.edu

Geoffrey Henebry

South Dakota State University, geoffrey.henebry@sdstate.edu

Braden C. Owsley

University of Oklahoma, bowsley@ou.edu

Irina N. Sokolik

Georgia Institute of Technology

Follow this and additional works at: https://openprairie.sdstate.edu/gsce_pubs

 Part of the [Climate Commons](#), [Environmental Studies Commons](#), [Physical and Environmental Geography Commons](#), and the [Remote Sensing Commons](#)

Recommended Citation

de Beurs, Kirsten M.; Henebry, Geoffrey; Owsley, Braden C.; and Sokolik, Irina N., "Large Scale Climate Oscillation Impacts on Temperature, Precipitation and Land Surface Phenology in Central Asia" (2018). *GSCE Faculty Publications*. 116.
https://openprairie.sdstate.edu/gsce_pubs/116

This Article is brought to you for free and open access by the Geospatial Sciences Center of Excellence (GSCE) at Open PRAIRIE: Open Public Research Access Institutional Repository and Information Exchange. It has been accepted for inclusion in GSCE Faculty Publications by an authorized administrator of Open PRAIRIE: Open Public Research Access Institutional Repository and Information Exchange. For more information, please contact michael.biondo@sdstate.edu.

Environmental Research Letters



LETTER

Large scale climate oscillation impacts on temperature, precipitation and land surface phenology in Central Asia

OPEN ACCESS

RECEIVED

12 January 2018

REVISED

10 May 2018

ACCEPTED FOR PUBLICATION

15 May 2018

PUBLISHED

14 June 2018

Kirsten M de Beurs^{1,4}, Geoffrey M Henebry², Braden C Owsley¹ and Irina N Sokolik³

¹ Department of Geography and Environmental Sustainability, University of Oklahoma, Norman, OK 73019, United States of America

² Geospatial Sciences Center of Excellence, South Dakota State University, Brookings, SD 57007, United States of America

³ School of Earth and Atmospheric Sciences, Georgia Institute of Technology, Atlanta, GA 30332, United States of America

⁴ Author to whom any correspondence should be addressed.

E-mail: kdebeurs@ou.edu

Keywords: land surface phenology, Central Asia, regional climate patterns, large scale climate oscillation

Original content from this work may be used under the terms of the [Creative Commons Attribution 3.0 licence](https://creativecommons.org/licenses/by/4.0/).

Any further distribution of this work must maintain attribution to the author(s) and the title of the work, journal citation and DOI.



Abstract

Central Asia has been rapidly changing in multiple ways over the past few decades. Increases in temperature and likely decreases in precipitation in Central Asia as the result of global climate change are making one of the most arid regions in the world even more susceptible to large-scale droughts. Global climate oscillations, such as the El Niño–Southern Oscillation, have previously been linked to observed weather patterns in Central Asia. However, until now it has been unclear how the different climate oscillations act simultaneously to affect the weather and subsequently the vegetated land surface in Central Asia. We fit well-established land surface phenology models to two versions of MODIS data to identify the land surface phenology of Central Asia between 2001 and 2016. We then combine five climate oscillation indices into one regression model and identify the relative importance of each of these indices on precipitation, temperature, and land surface phenology, to learn where each climate index has the strongest influence. Our analyses illustrate that the North Atlantic Oscillation, the East Atlantic/West Russia pattern, and the Atlantic Multi-Decadal Oscillation predominantly influence temperature in the northern part of Central Asia. We also show that the Scandinavia index and the Multivariate ENSO index both reveal significant impacts on the precipitation in this region. Thus, we conclude that the land surface phenology across Central Asia is affected by several climate modes, both those that are strongly linked to far northern weather patterns and those that are forced by southern weather patterns, making this region a ‘climate change hotspot’ with strong spatial variations in weather patterns. We also show that regional climate patterns play a significant role in Central Asia, indicating that global climate patterns alone might not be sufficient to project weather patterns and subsequent land surface changes in this region.

Introduction

Central Asia is one of the most arid regions in the world with a large fraction of the population relying directly on agriculture and pastoralism, making these people especially vulnerable to drought (Reyer *et al* 2017). The land surface of Central Asia has experienced tremendous changes over the last three decades both as a result of human impacts and due to a changing and variable climate. The predominant human driven change was the fundamental transformation of agricultural systems across large swaths of the land surface as a result of the collapse of the Soviet Union between 1991 and 2000 (de Beurs *et al* 2015, Lioubimtseva *et al* 2015,

de Beurs and Henebry 2004), followed by a period of recovery (Lioubimtseva *et al* 2015, Lioubimtseva *et al* 2013). The area is still affected by land degradation as a result of abandonment in some areas (Tüshaus *et al* 2014), as well as a result of salinization in other regions (Sommer *et al* 2013). Climate models are predicting increases in temperature and decreases in summer precipitation in the western part of Central Asia (Lioubimtseva 2015, Lioubimtseva *et al* 2015) with slight increases in winter precipitation in the eastern, more mountainous regions (Lioubimtseva *et al* 2015, Hu *et al* 2016). In fact, increases in temperature and decreases in precipitation are already evident, especially in the western part of Central Asia (Lioubimtseva *et al*

2015, Hu *et al* 2016), making the region increasingly prone to droughts (Barlow *et al* 2016). For example, the hot summer of 2010 provides an example of a ‘mega-heatwave,’ occurrences which are predicted to increase by a factor of 5–10 (Barriopedro *et al* 2011). This particular heat event at least partly resulted from a strong deficit of January to July precipitation, and the resulting lack of water availability exacerbated the strength of the heat wave (Barriopedro *et al* 2011). While the major heat dome was located north of Central Asia, Kazakhstan was affected by increased temperatures, breaking summer heat records.

We have defined land surface phenology as the spatio-temporal pattern of the vegetated land surface as observed by synoptic sensors (de Beurs and Henebry 2004, de Beurs and Henebry 2005, Henebry and de Beurs 2013). We have previously shown that land surface phenology metrics can be used to demonstrate the effect of large scale institutional changes (de Beurs and Henebry 2004), as well as changes resulting from climate impacts (e.g. de Beurs and Henebry 2010). In Central Asia, land surface phenology has been linked with climate and winter, spring and summer precipitation have been shown to be strong drivers of the land surface phenology (Kariyeva *et al* 2012, Kariyeva and van Leeuwen 2011). Temperature was shown to affect spring and peak vegetation timing, and higher temperatures were linked to a decrease in vegetation productivity (Kariyeva *et al* 2012). Temperature was also found to be a main driver for mountainous vegetation variability as well as vegetation variability on irrigated lands (Dubovyk *et al* 2016). Some have argued that the relative importance of climatic variables and land management practices should be analyzed in more detail (Dubovyk *et al* 2016).

Large scale climate oscillations have been demonstrated to correlate directly with both temperature and precipitation, which, in turn, influence land surface properties such as land surface phenology (Hurrell 1995, Barlow *et al* 2002, Syed *et al* 2006, Deser *et al* 2012). We have previously shown that fluctuations in land surface phenology in the northern hemisphere can be linked significantly to the Northern Atlantic Oscillation as well as the Arctic Oscillation (de Beurs and Henebry 2010, de Beurs and Henebry 2008). In addition, we earlier demonstrated that the North Atlantic Oscillation (NAO) significantly impacts the land surface in the northern portions of Central Asia (Wright *et al* 2014), being at least partly responsible for the 2010 heat wave that significantly affected agricultural production. Some have argued that this heat wave and the coinciding major flooding that occurred in Pakistan were meteorologically connected (Lau and Kim 2012).

Several studies have identified significant effects from a diverse set of climate oscillation patterns on precipitation and temperature in Central Asia. For example, some have speculated that the prolonged La Niña between 1998 and 2001 resulted in extraordinary droughts in the region during those years (Barlow

et al 2002), and that both NAO and the El Niño–Southern Oscillation (ENSO) play a significant role in winter precipitation in the southern parts of Central Asia (Syed *et al* 2006). As a result, it is perhaps not surprising that (Chen *et al* 2016) identified a significant correlation between El Niño (NINO4) and burned areas in the grasslands of Central Asia. Others indicate that the warm phase of the Atlantic Multidecadal Oscillation (AMO) can significantly affect the Indian monsoon rainfall, which affects the southern part of Central Asia (Li *et al* 2008). Yet others found that the Scandinavian (SCAND) and East Atlantic/West Russia (EAWR) patterns reveal the most significant effect on regional precipitation in the southeastern part of Central Asia (Bothe *et al* 2012).

Here our goal is to understand how the different climate oscillations act simultaneously to affect the weather and subsequently the land surface phenology. We first determine the correlation between large scale climate oscillations and a set of climate variables. Instead of analyzing one or two of the most prevalent indices as presented in the literature, we simultaneously analyze five climate oscillations that have been shown to affect the region. We use correlation-adjusted correlation (CAR) scores to determine the relative importance of each of the indices on the landscape (Zuber and Strimmer 2011). We also link the most significant climate oscillations directly with land surface phenology metrics focused on growing season productivity using CAR scores. Collection 6 of the MODIS data was released in the fall of 2015. Some papers have highlighted significant sensor degradation in collection 5 and notable differences between time series in collections 5 (V005) and 6 (V006) (Wang *et al* 2012, Zheng and Zhu 2017, Lyapustin *et al* 2014). In this paper we evaluate the land surface phenology for these two collections, and we investigate how well the land surface phenology results from the two collections correlate with large scale climate indices. As described above, global climate oscillations have previously been linked to observed weather patterns in Central Asia. However, until now it has been unclear how the different climate oscillations interact to affect precipitation and temperature and subsequently the vegetated land surface in Central Asia.

Study region

We identify Central Asia as the region including five countries: Kazakhstan, Kyrgyzstan, Tajikistan, Turkmenistan, and Uzbekistan. The total area is approximately 4 million km² with climate ranging from cold drylands and dryland forests in the north to dry, hot deserts in the south. The annual average rainfall in the region ranges from 100 mm in central Kazakhstan around the Caspian Sea to about 550 mm in the montane areas of Tajikistan. The population density in Central Asia ranges from virtually no people per

km² in desert areas to as many as 12 000 people per km² in the Ferghana Valley of Uzbekistan (Dobson *et al* 2000). The total population in 2015 was about 68.5 million, with the majority of people in Uzbekistan (31 million), which also has the highest average population density (69 km⁻²), followed by Tajikistan (60 km⁻²). Kazakhstan has the lowest average population density of 6.3 km⁻².

Data

Climate oscillation data

We analyze the effect of five different climate oscillation patterns that have been identified as impacting the land surface in Central Asia. The SCAND pattern, also identified as Eurasia-1, has been shown to significantly affect spring temperatures over central Eurasia (Barnston and Livezey 1987). The East Atlantic/West Russia pattern (EAWR) is also identified as the Eurasia-2 pattern (Barnston and Livezey 1987). The positive phase of EAWR is associated with below average temperatures in Western Russia. Besides these two climate patterns that are specifically linked to Eurasia, we also investigate the Atlantic Multi-Decadal Oscillation (AMO, Schlesinger and Ramankutty (1994), the North Atlantic Oscillation NAO Hurrell (1995), and the El Niño-Southern Oscillation (ENSO). We use the Multivariate ENSO Index (MEI, Wolter and Timlin 1998) to track the ENSO dynamics. The AMO is variability expressed in sea surface temperatures in the North Atlantic Ocean. AMO is a multi-decadal oscillation that has been predominantly in a positive phase since the late 1990s (Schlesinger and Ramankutty 1994).

The NAO, EAWR, and SCAND indices were obtained from the National Weather Service Climate Prediction Center (Climate Prediction Center 2018). AMO was obtained from NOAA's Earth System Research Laboratory (Earth System Research Laboratory 2018a). The MEI is based on six variables observed over the Pacific Ocean. This time series was also downloaded from NOAA's Earth System Research Laboratory (2018b). Each climate index, except MEI, was provided as a monthly index, which we summarized into seasonal indices by calculating the average for winter (DJF), spring (MAM) and summer (JJA). MEI was provided as a bimonthly index (e.g. DEC-JAN), which we summarized in similar seasons as the other indices. We are not presenting the results for the fall season, because we are interested in the potential predictive capability of the climate indices on the peak of the growing season, which for this area occurs in the late spring or summer. An overview of the spring indices (MAM) since 2001 can be found in figure 1. Table 1 provides the Spearman correlation between these individual indices. A significant negative correlation is revealed between spring AMO, NAO and EAWR indices. There is a significant positive correlation

between NAO and EAWR. Since for each index we provide the correlation of three different seasons (DJF, MAM and JJA), table 1 also reveals the autocorrelation between the different seasons. For example, the autocorrelation between EAWR in winter (DJF) and spring (MAM) is 0.40, and we find a significant autocorrelation of 0.48 between spring and summer. The slow moving AMO index reveals the most consistent seasonal autocorrelation, with significant autocorrelations between AMO in winter and spring (0.50) and in spring and summer (0.58). The MEI also reveals a significant correlation between winter and spring (0.74).

Gridded precipitation and temperature data (2001–2016)

We obtained high-resolution gridded temperature and precipitation data from the Climatic Research Unit (CRU TS v.4.01), which covers all global land areas monthly at 0.5° resolution (Harris *et al* 2014, Harris and Jones 2017). While we only present results based on mean temperature (tmp) and mean precipitation (pre), we also tested our analyses for the minimum and maximum temperatures (tmn and tmx). We summarized all the monthly data into seasonal averages for precipitation and temperature maintaining the same seasons as described for the climate indices.

MODIS Nadir BRDF-adjusted reflectance (NBAR) and land surface temperature Data

We used the MODIS MCD43C4 NBAR collection 5 and collection 6 (V005/V006) products to determine the Normalized Difference Vegetation Index (NDVI) for each eight-day period between 2001 and 2016. This dataset is produced at 0.05° spatial resolution. The MCD43C4 product is a nadir BRDF (bidirectional reflectance distribution function)-adjusted reflectance product that we have used in several previous studies to determine the land surface phenology (de Beurs and Henebry 2008, de Beurs *et al* 2015). Each eight-day observation is based on 16 d of data that are used to create the BRDF model (Schaaf *et al* 2002, Liu *et al* 2016). Besides the optical data, we also use MODIS Land Surface Temperature data (MOD11C2). This dataset is also delivered at the 0.05° spatial resolution and eight-day time step. For each year and time step, we first calculated the growing degree-days as follows, where we set the growing degree-days to zero if the average between the day and night temperature is less than 0 °C:

$$\text{GDD} = \frac{\text{Temp}_{\text{day}} + \text{Temp}_{\text{night}}}{2} > 0. \quad (1)$$

In a subsequent step, we summed the number of growing degree-days for each composite by year to create an annual accumulated growing degree-day product:

$$\text{AGDD}_t = \text{AGDD}_{t-1} + \text{GDD}_t \quad (2)$$

where, for $t = 1$, the $\text{AGDD}_t = \text{GDD}_t$.

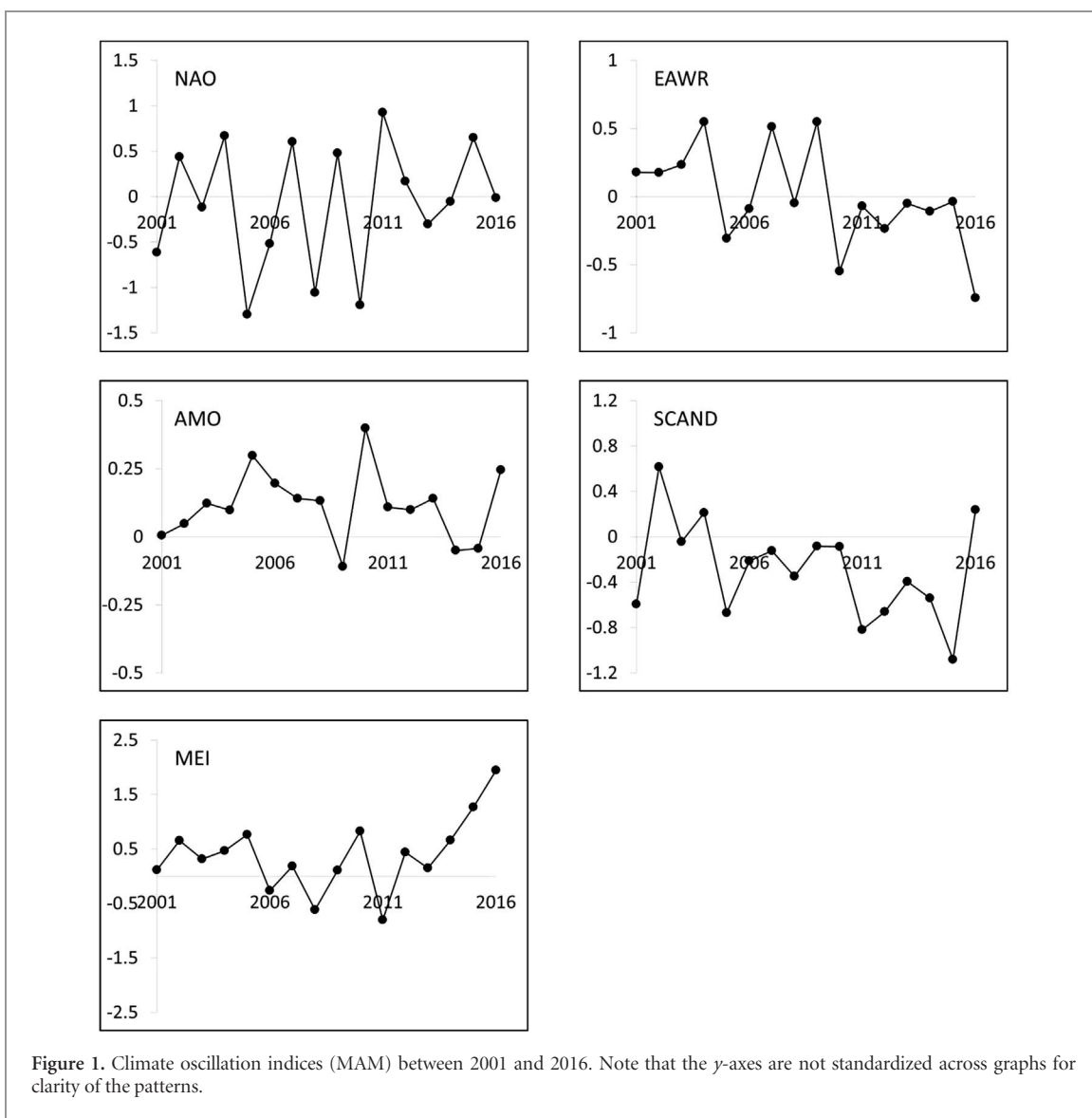


Figure 1. Climate oscillation indices (MAM) between 2001 and 2016. Note that the y-axes are not standardized across graphs for clarity of the patterns.

Table 1. Spearman correlation between the climate oscillation indices. Bold indicates $p < 0.10$, * indicates $p < 0.05$.

		NAO			EAWR			AMO			SCAND			MEI	
		DJF	MAM	JJA	DJF	MAM	JJA	DJF	MAM	JJA	DJF	MAM	JJA	DJF	MAM
NAO	MAM	-0.01	1.00												
	JJA	-0.29	-0.32	1.00											
EAWR	DJF	0.17	-0.01	0.47	1.00										
	MAM	-0.32	0.46	0.32	0.40	1.00									
AMO	JJA	0.24	0.18	-0.26	0.11	0.48	1.00								
	DJF	0.01	0.29	0.20	0.36	-0.08	-0.55*	1.00							
SCAND	MAM	-0.08	-0.51*	0.16	0.19	-0.55*	-0.58*	0.50	1.00						
	JJA	0.03	-0.59*	-0.09	-0.11	-0.61*	-0.31	0.00	0.58*	1.00					
MEI	DJF	-0.36	-0.59*	0.10	-0.43	-0.31	-0.08	-0.59*	0.11	0.40	1.00				
	MAM	-0.27	0.06	0.36	0.29	0.26	-0.29	0.39	0.12	0.13	-0.22	1.00			
MEI	JJA	-0.24	-0.17	0.15	-0.02	-0.13	-0.11	0.09	0.09	-0.24	0.19	-0.19	1.00		
	DJF	0.06	-0.15	0.33	0.23	-0.16	-0.51*	0.40	0.49	0.32	-0.20	0.41	-0.41	1.00	
MEI	MAM	0.47	-0.05	0.00	-0.05	-0.40	-0.37	0.20	0.14	0.30	-0.27	0.15	-0.46	0.74*	1.00
	JJA	0.53*	0.30	-0.18	-0.10	0.18	0.44	-0.34	-0.68*	-0.15	-0.16	-0.09	-0.23	-0.23	0.23

Methods

Land surface phenology

We used AGDD and NDVI to create annual land surface phenology models by fitting a simple quadratic model for each pixel as follows:

$$\text{NDVI} = \alpha + \beta\text{AGDD} - \gamma\text{AGDD}^2$$

where α , β and γ are the quadratic parameters fit. To find the best fitting model, we started with the longest possible duration, which in this case consists of 468 day observations. In subsequent steps, we decreased the number of observations included, e.g. from 46 to 45, to 44, and so forth. In addition, we shifted the shorter candidate models within the available time period, e.g. there are two possible candidates for a model with length 45 (1–45 and 2–46). We repeated this procedure of shrinking the model duration, and shifting the candidate models along the available period until we found a model with an adjusted coefficient of determination (R^2_{adj}) larger than our predefined threshold of 0.90 (figure 2). If no model with an R^2_{adj} was found for a particular pixel, the model with the highest R^2_{adj} and a minimum length of ten observations (80 d) was selected. We repeated this procedure at each pixel for each year. Once we had a well-fitting model at each pixel for each year, we used the fitted parameter coefficients to calculate 1) the number of accumulated growing degree-days necessary to reach the peak of the growing season (figure 2), which we labeled ‘thermal time to peak’ (TTP) and 2) the NDVI value at the peak of the growing season, which we labeled ‘peak height’ (PH). The peak height typically fluctuates with droughts, e.g. higher temperatures and/or lower precipitation amounts. In a year with lower amounts of precipitation, the peak height tends to be lower, because the growing season is less productive. The peak height can also change as a result of anthropogenic change. For example, crop changes or changes in irrigation patterns can have an effect on the peak height. Population increases leading to urban expansion and increases in the impervious surface can also affect peak height. The final result consisted of 16 separate maps of TTP and PH across the study region, one for each year from 2001–2016.

Spearman rank correlation

Spearman rank correlation allows for correlations that are not linear and is relatively robust against outliers (Lehmann and D’Abrera 1998). We used the Spearman rank correlation to test a variety of different relationships.

1. We calculated the Spearman correlation between the mean spring and summer temperatures and precipitation and each of the winter, spring, and summer climate indices (e.g. NAO/JJA).

2. We linked the PH with each of three seasons for each of five climate oscillation indices, resulting in a series of 15 maps for PH, one for each season/climate oscillation combination (e.g. DJF/NAO), for each MODIS version (V005/V006).

For each final map, we calculated the percentage of pixels with a significant correlation ($p < 0.10$).

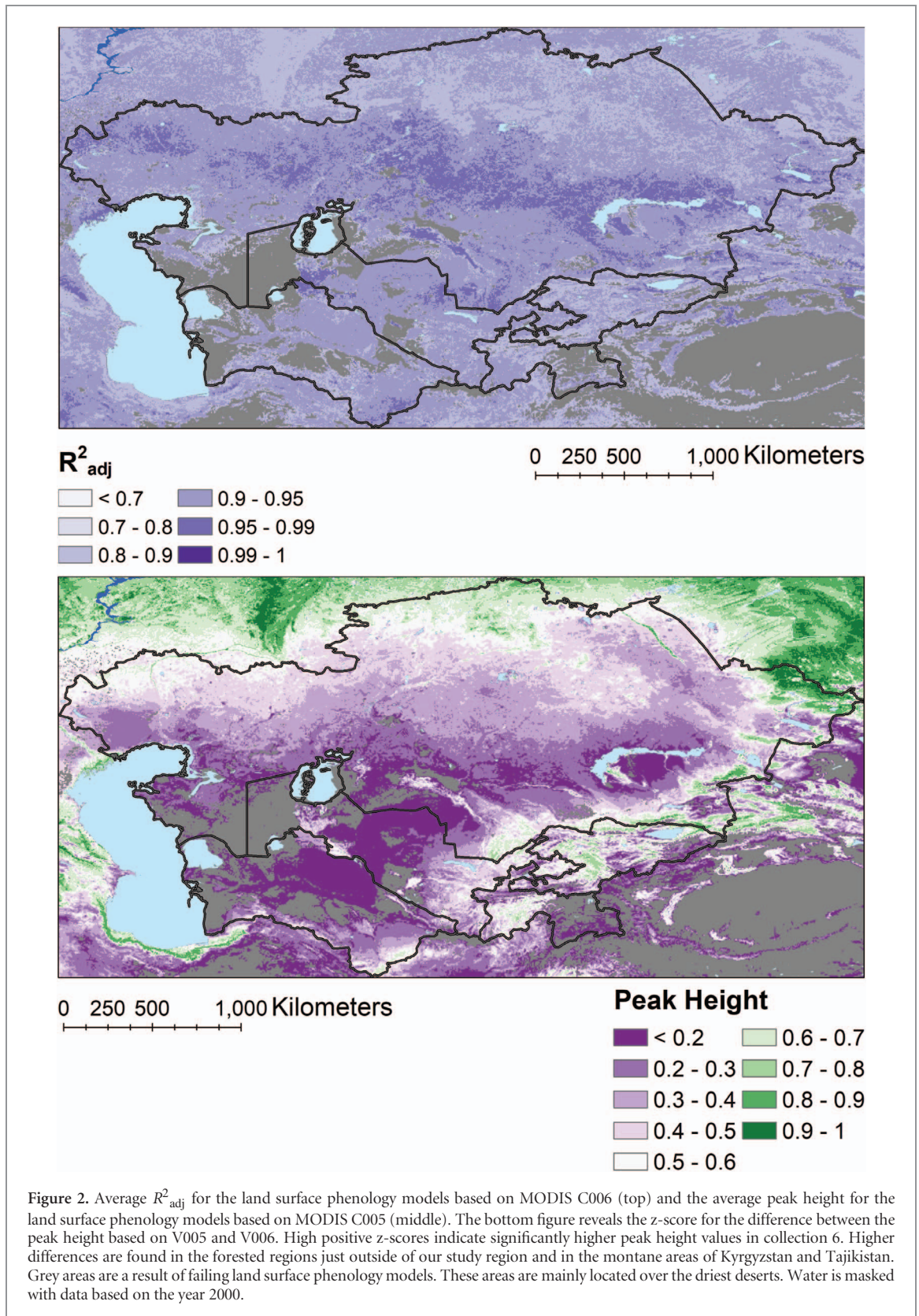
Multiple linear regression

Finally, we used as independent variables in a multiple linear regression model, every climate oscillation index that showed a significant correlation with PH in at least 10% of the Central Asian land surface. To determine the best fitting model, we tested all combinations of regression models, e.g. ranging from a model incorporating every independent variable, to models incorporating just one independent variable. We then ranked the models according to their R^2_{adj} and, for each pixel, we selected the model with the highest R^2_{adj} .

For each pixel and variable, we also determined the CAR score, which is a criterion for variable ranking in linear regression based on the Mahalanobis-decorrelation (Zuber and Strimmer 2011). The method to determine the CAR score uses the marginal correlations adjusted for the correlation among explanatory variables, which is useful in this case because some climate indices are correlated (table 1). CAR scores have been effective both in small and large sample cases and can also be used when the number of variables is much larger than the number of observations (Bocinsky and Kohler 2014). Since we applied these multiple linear regression models by pixel, each model was based on just 16 observations (2001 through 2016) and up to seven climate indices (e.g. including those from different seasons) as explanatory variables. CAR scores may ultimately be viewed as a variation of the partial correlation coefficients specifically tuned for multivariate situations with correlated variables (Zuber and Strimmer 2011). We present maps of CAR scores for each climate oscillation index that revealed significant correlations across at least 10% of the land surface.

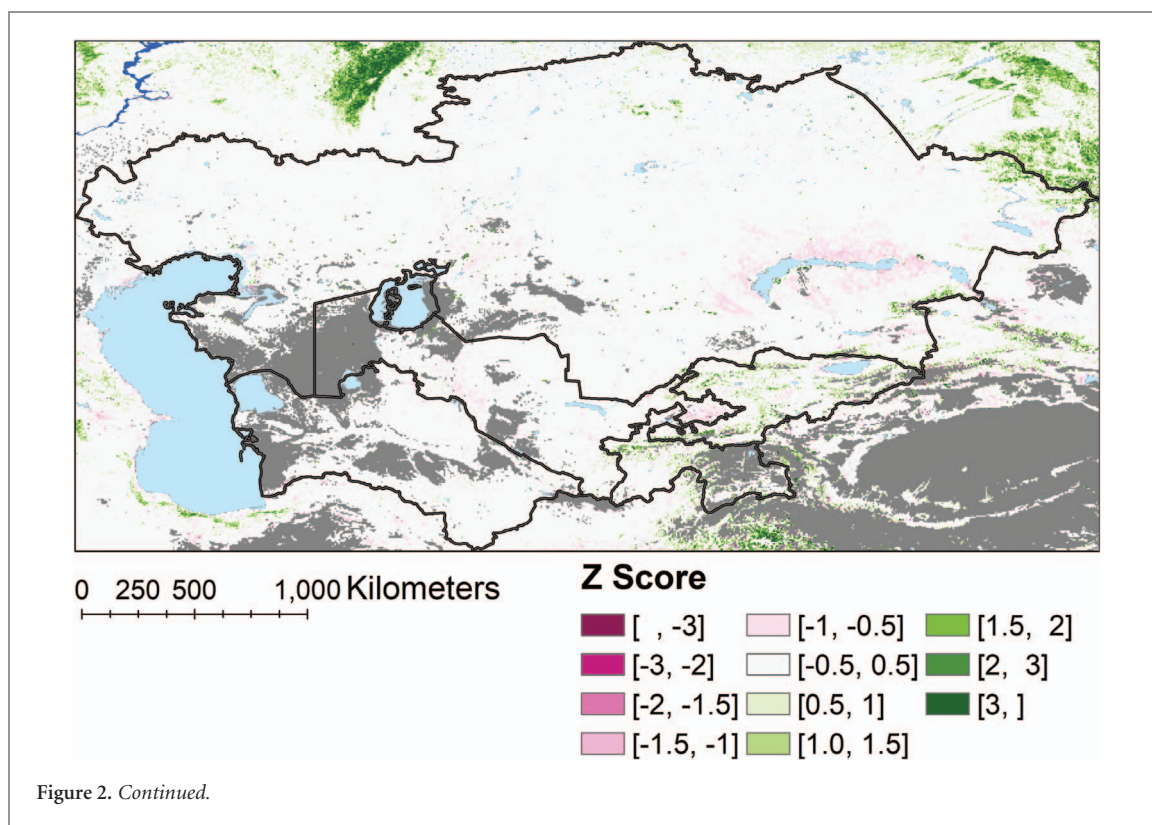
Results and discussion

We evaluate the results of the land surface phenology model for Central Asia by analyzing the R^2_{adj} , which summarizes the fit for the quadratic model. We masked approximately 12% of the pixels for the models from both collection 5 (11.5%) and collection 6 (12.4%), where the pixels were open water or where the annual variability in NDVI was so low that we were unable to find a well-fitting model. The combined mask for both collections covered 13.45% (541 575 km²) of the study area. After masking the regions with no model, which are mainly found in the driest deserts, we found that for both collections, 75% (2 613 757 km²) of the



study area revealed an average model fit with an R^2_{adj} of at least 0.90, and 99.7% (3 474 554 km²) of the study area had an average R^2_{adj} of at least 0.80. These results indicate that the quadratic models fit the observed land surface phenology very well (figure 2). Note that the differences in model fits between V005 and V006 were so small that we only present figures for V006.

The average PH over the 16 years (figure 2) reveals an expected north-south pattern over Central Asia, with higher NDVI at the peak of the growing season for the northern wheat growing regions of Kazakhstan, gradually declining toward the more arid areas. The riparian irrigated areas around the Syr Darya and the Amu Darya in southern Kazakhstan and northwestern Uzbekistan



also reveal moderate NDVI values, as do the highland pastures and croplands of Kyrgyzstan and Tajikistan. Higher PH values are also found in the crop growing region of southern Turkmenistan at the Afghanistan border. The results are almost identical between V005 and V006 for most of our study region with the Z-scores close to 0, except for the forested regions just north of Kazakhstan, where a significantly higher PH is found for V006, with Z-scores above 2 (figure 2).

Univariate climate oscillation impacts on precipitation and temperature

Tables 2 and 3 report the percentage of land area significantly affected by any of the five climate indices. We analyzed the effect of each of these climate indices individually, e.g. without considering the impact of any other index. We first present the correlation results for spring temperature and precipitation with winter and spring climate indices. AMO, EAWR and NAO each exert significant influence on spring temperature over more than 10% of the study area, with the most widespread effects (>48%) being a negative correlation between temperature and the spring EAWR and spring NAO indices (table 2). Both SCAND and MEI associate with precipitation effects across a broad area: the winter MEI and spring SCAND indices are each positively correlated with spring precipitation for nearly half of the study area, and spring MEI is positively correlated with more than a quarter of the land area (table 2). The general pattern in the summer reveals that AMO, EAWR, and NAO primarily affect temperature,

whereas SCAND and MEI primarily affect precipitation (table 3). However, spring SCAND has a significant negative influence on summer temperatures in more than half of the land surface, perhaps linked to the precipitation response in the spring. For example, when spring SCAND is highly positive, spring precipitation is above average (significant positive correlation for 49% of the land surface, table 2), and summer temperature is below average (significant negative correlation for 50% of the land surface). While there is a strong correlation between winter and spring MEI and spring precipitation, the relation between these indices and summer precipitation is much weaker.

Univariate climate oscillation impact on land surface phenology

Since we are evaluating five different climate oscillation indices (AMO, EAWR, NAO, SCAND, MEI), during three different seasons (DJF, MAM, JJA) and two different collections (5 and 6), there are 30 ($5 \times 3 \times 2$) different mapping combinations. For each of the combinations, we investigate whether the correlation between the climate index and phenological metric is significant ($p < 0.10$). Table 4 reports the total percentage of land area with a significant correlation between the peak height of the growing season as measured by NDVI and the climate oscillation index during any season.

Table 4 reveals very similar patterns in the correlations between V005 and V006. Both collections reveal the largest percentage of significant correlation between

Table 2. (a) Percentage of land area and (b) land area in 1000 km² exhibiting Spearman correlation between seasonal (winter or spring) climate oscillation index and either spring temperature or spring precipitation. Numbers in bold indicate correlation is significant at $p < 0.10$ across at least 10% of the study area.

(a) Area %	SPRING	DJF		MAM	
		-	+	-	+
AMO	Temperature	0	<1	0	18
	Precipitation	0	14	3	3
EAWR	Temperature	0	0	48	0
	Precipitation	<1	1	0	5
NAO	Temperature	0	29	49	0
	Precipitation	2	0	0	12
SCAND	Temperature	0	<1	0	0
	Precipitation	17	0	0	49
MEI	Temperature	<1	0	<1	0
	Precipitation	<1	49	1	28
(b) Area 1000 km ²	SPRING	DJF		MAM	
		-	+	-	+
AMO	Temperature	0	2	0	707
	Precipitation	0	566	119	102
EAWR	Temperature	0	0	1940	0
	Precipitation	9	50	0	212
NAO	Temperature	0	1146	1979	0
	Precipitation	95	0	0	490
SCAND	Temperature	0	030	0	0
	Precipitation	683	0	0	1977
MEI	Temperature	33	0	26	0
	Precipitation	37	1963	58	1112

Table 3. (a) Percentage of land area and (b) land area in 1000 km² exhibiting Spearman correlation between seasonal (winter or spring or summer) climate oscillation index and either temperature or precipitation in summer. Numbers in bold indicate correlation is significant at $p < 0.10$ across at least 10% of the study area.

(a) Area %	SUMMER	DJF		MAM		JJA	
		-	+	-	+	-	+
AMO	Temperature	0	0	0	2	0	19
	Precipitation	<1	12	<1	3	<1	2
EAWR	Temperature	15	0	81	0	<1	0
	Precipitation	0	4	<1	<1	1	<1
NAO	Temperature	0	56	0	0	89	0
	Precipitation	1	<1	<1	2	<1	6
SCAND	Temperature	<1	0	50	0	<1	0
	Precipitation	8	0	3	19	14	0
MEI	Temperature	4	0	0	0	0	0
	Precipitation	0	17	<1	6	1	0
(b) Area 1000 km ²	SUMMER	DJF		MAM		JJA	
		-	+	-	+	-	+
AMO	Temperature	0	0	0	100	0	784
	Precipitation	15	486	4	102	37	95
EAWR	Temperature	594	0	3266	0	0	0
	Precipitation	0	154	17	13	46	24
NAO	Temperature	0	2239	0	0	3586	0
	Precipitation	56	37	6	63	26	230
SCAND	Temperature	15	0	2026	0	17	0
	Precipitation	308	0	132	765	581	0
MEI	Temperature	147	0	0	0	0	0
	Precipitation	0	670	28	256	58	0

Table 4. (a) Percentage of land area and (b) land area in 1000 km² exhibiting Spearman correlation between seasonal (winter or spring or summer) climate oscillation index and the peak height from either MODIS collection 5 or 6. Numbers in bold indicate correlation is significant at $p < 0.10$ across at least 10% of the study area. Data with ill-fitting models were masked and data were constrained to only the pixels in the Central Asia countries in the study area.

(a) Area %		DJF		MAM		JJA	
		-	+	-	+	-	+
AMO	V005	<1	18	1	4	10	2
	V006	<1	18	1	5	10	2
EAWR	V005	1	14	3	8	6	1
	V006	2	10	4	5	7	<1
NAO	V005	1	7	<1	7	<1	14
	V006	<1	9	<1	8	1	10
SCAND	V005	28	<1	<1	28	15	2
	V006	26	<1	<1	25	16	2
MEI	V005	<1	36	<1	26	1	3
	V006	<1	35	<1	29	1	4
Area 1000 km ²		DJF		MAM		JJA	
		-	+	-	+	-	+
AMO	V005	5	638	52	153	351	70
	V006	6	630	52	165	334	76
EAWR	V005	37	489	93	261	226	41
	V006	75	350	144	183	258	30
NAO	V005	42	248	18	235	24	478
	V006	35	301	14	286	51	342
SCAND	V005	964	6	15	973	537	70
	V006	921	7	19	878	551	60
MEI	V005	12	1265	25	922	39	122
	V006	11	1227	23	1004	38	136

the winter and spring MEI and the peak of the growing season, followed by winter and spring SCAND indices. The next most important climate index was the winter AMO index, which reveals a significant positive correlation with the NDVI peak height in 18% of the land area (V005). Most other combinations reveal smaller areas with significant correlations (<10%), with the exception of the slightly larger percentages of significant correlations between winter EAWR and the peak height (14%, 10%), and summer NAO and the peak height (14%) in V005.

Multivariate climate oscillation impacts on weather and land surface phenology

Figure 3 provides the R^2_{adj} for the multiple regression model between all significant climate indices (table 4) and the peak height of the growing season (V006). Most of the significant correlations can be found in the central portion of Kazakhstan with other significant models in the southern parts of Central Asia. Note that the northern wheat growing region of Kazakhstan shows no significant multi-regression model with the climate indices (areas in white on figure 3). We expect that this results from the direct human influence on cultivation and fallow periods, which directly affects the NDVI peak height. As a result of the relatively short study period (16 years), other fluctuations such as

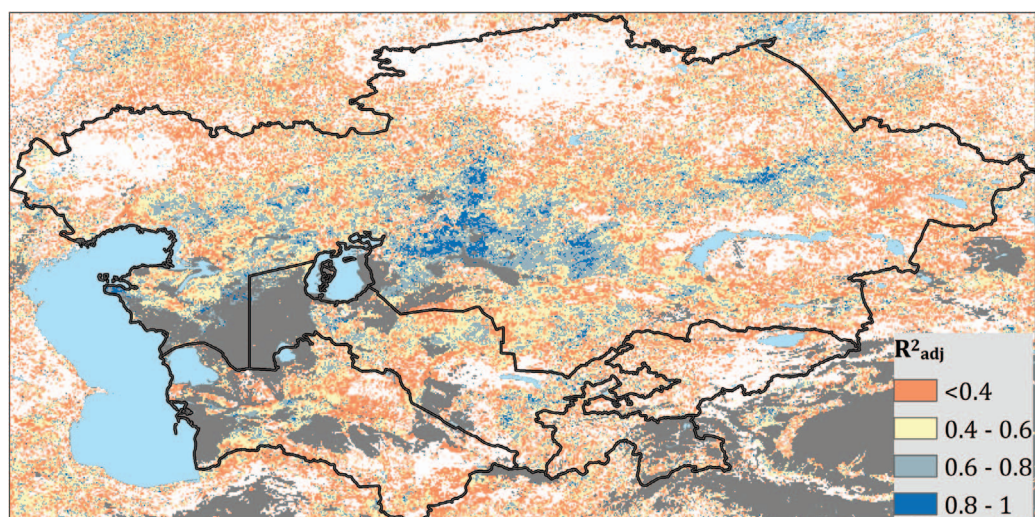


Figure 3. The R^2_{adj} for the models with peak height as the response variable and the climate oscillation indices as the independent variables reveals that the climate oscillation variables explain more than 40% of the variability in the peak height for much of the area of Central Asia. White regions are areas where the p-value of the best fitting model is greater than 0.05, indicating that no significant model was found combining any of the climate indices as explanatory variables. Dark grey areas were excluded from the analysis due to extreme aridity/lack of vegetation signal.

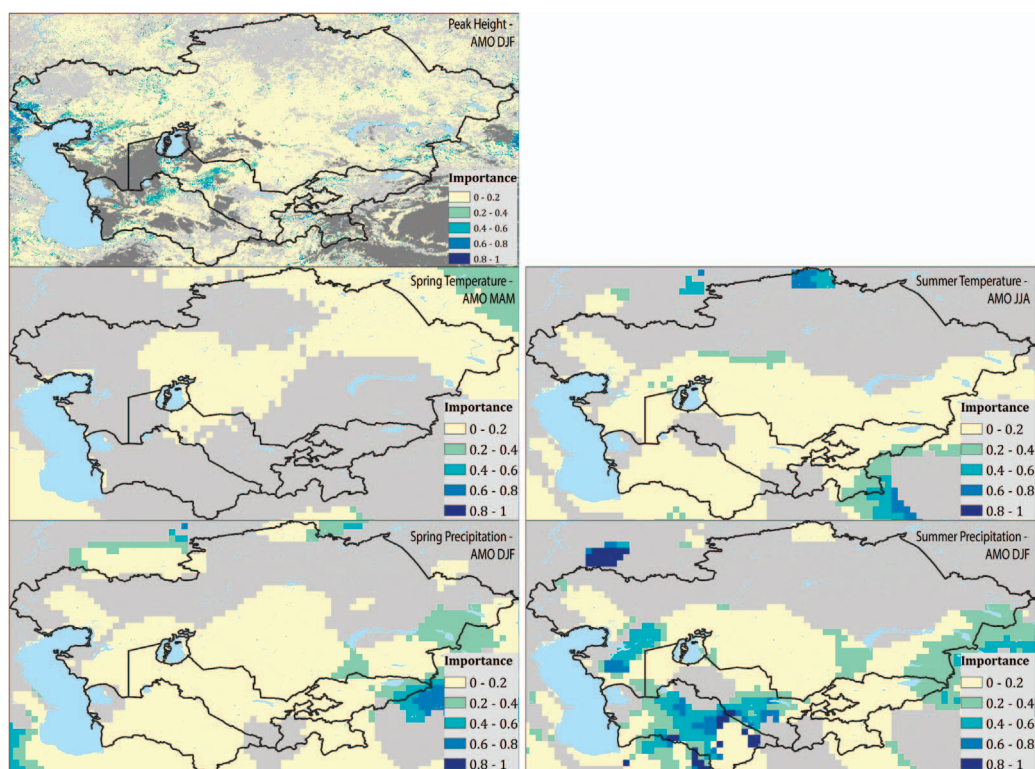


Figure 4. Impact of the AMO index on the summer and spring temperature, as well as the summer and spring precipitation. Most of AMO's influence on the NDVI peak height is visible in the southwestern part of Central Asia, mainly driven by AMO's influence on summer precipitation.

human impacts can significantly impact the land surface phenology and, consequently, impact the strength of the correlation (de Beurs and Henebry 2004, de Beurs and Ioffe 2014). (Kariyeva *et al* 2012) also demonstrated that the relationship between temperature and precipitation variables with land surface phenology is less clear in areas dominated by irrigated agriculture.

Interestingly, for our short time period of 16 years, we find stronger correlations between the climate indices and the land surface phenology in the irrigated regions than in the northern, rain-fed croplands. We suspect that lower correlations are visible in these northern croplands as a result of the prevalence of hard fallow periods, where there are no crops on the land,

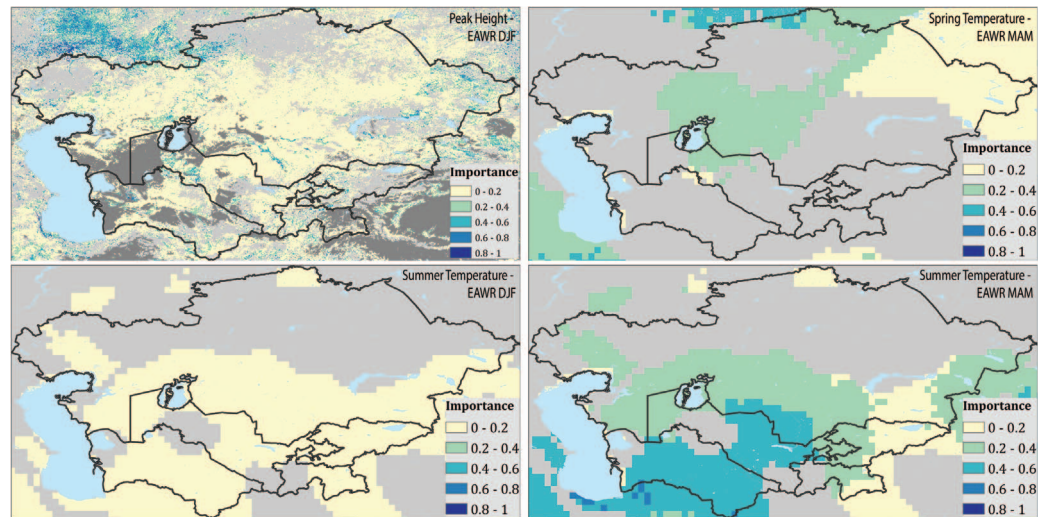


Figure 5. Impact of the EAWR index on the spring and summer temperature, as well as the NDVI peak height. It is interesting to note that while EAWR significantly impacts the land surface phenology just northwest of Kazakhstan, EAWR is less important for the temperature in that area.

that change the final correlations (de Beurs and Ioffe 2014). Figures 4 through 8 present the CAR scores or importance results for each climate oscillation index. Note that these figures correspond to the highlighted results in tables 2–4. For example, in figure 4 we are revealing the effect of the AMO index. For MODIS V006, AMO is most significant in the winter (DJF; 18%, table 4). In addition, we find a significant correlation between spring AMO and spring temperature (18%, table 2), as well as winter AMO and spring precipitation (14%, table 2), summer AMO and summer temperature (19%, table 3) and winter AMO and summer precipitation (12%, table 3). Figure 4 reveals where each of these effects are important. Grey areas indicate no significant relationship with a particular index. Note that while AMO affects both temperature and precipitation in both the spring and the summer, these effects translate to relatively small impacts on the NDVI peak height. The EAWR index predominantly affects temperature and most effects are visible in the eastern part of our study region, as well as just north of our actual study region (figure 5). The EAWR dipole pattern consists of two anomalous atmospheric centers, with one located over the Caspian Sea (Kazmin and Zatssepina 2007). Characteristics of the EAWR have been found to resemble the North-Sea Caspian Pattern (Kutiel and Benaroch 2002, Oguz *et al* 2006), which has been found to correlate with summer temperatures in many areas of Europe, including regions as far southeast as our study region. Significant negative correlation was found in the area corresponding closely with our identified region of importance just northwest of Kazakhstan (Brunetti and Kutiel 2011). Others have found that the combination of the NAO and EAWR is effective in explaining climate-induced variability in the Black Sea region (Krichak *et al* 2002, Oguz *et al* 2006). We found that NAO and EAWR

predominantly influence temperature, and while their regions of importance overlap, their strongest zones of importance are not co-located. (Krichak *et al* 2002) found that the combination of these two indices had a strong influence on precipitation just west of our study region, in the Mediterranean.

NAO in both winter and summer affects both spring and summer temperatures, with the most visible effects on the land surface phenology in the northern part of our study area (figure 6). The winter NAO has a particularly strong impact on the spring temperature in the northeastern part of the study area, which is also reflected clearly in the correlation between the NDVI peak height and the summer NAO. Phenology in the far northern latitudes is strongly affected by the NAO, and these effects are visible in the northern parts of Central Asia as well (de Beurs and Henebry 2008, Stöckli and Vidale 2004, Li *et al* 2016).

The SCAND index and the MEI reveal strong impacts on both spring and summer precipitation, with a significant impact on the NDVI peak height in central Kazakhstan and farther south (figures 7 and 8). Note that the MEI influences the land surface phenology in central Kazakhstan and that the strongest influence of SCAND is just south of that region (figure 7 and 8). We also found that SCAND and MEI significantly influence the land surface phenology in Uzbekistan and Turkmenistan (Kariyeva and van Leeuwen 2012), although again the spatial location where these indices are most important is slightly offset for these indices. Figure 7 and 8 demonstrate that both indices are primarily affecting precipitation. Two of the most severe regional droughts were during strong La Niña conditions in 1999–2001 and 2007/08 (Barlow *et al* 2016), likely driving our strong correlation patterns. However, few papers have analyzed the effect of these climate indices on smaller drought episodes (Barlow *et al* 2016).

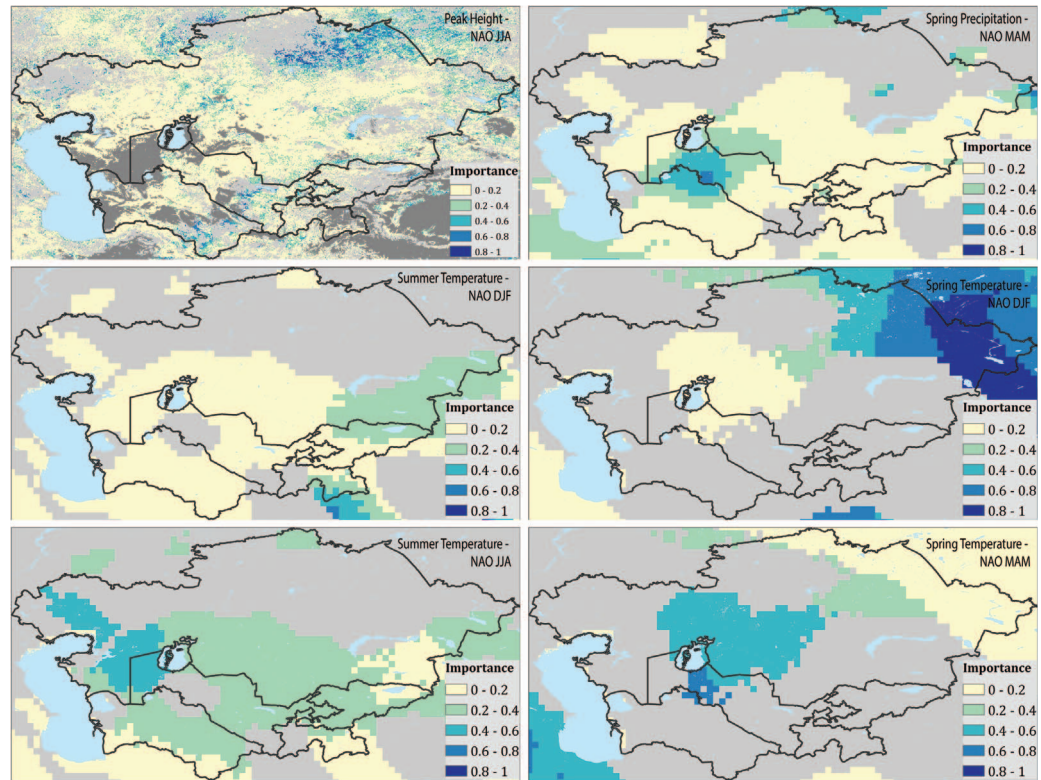


Figure 6. Impact of the NAO index on the spring and summer temperature, as well as the spring precipitation and the NDVI peak height. The impact on the peak height is mainly visible in the northeastern part of Kazakhstan, corresponding with a significant impact of the winter NAO index on the spring temperature in this region.

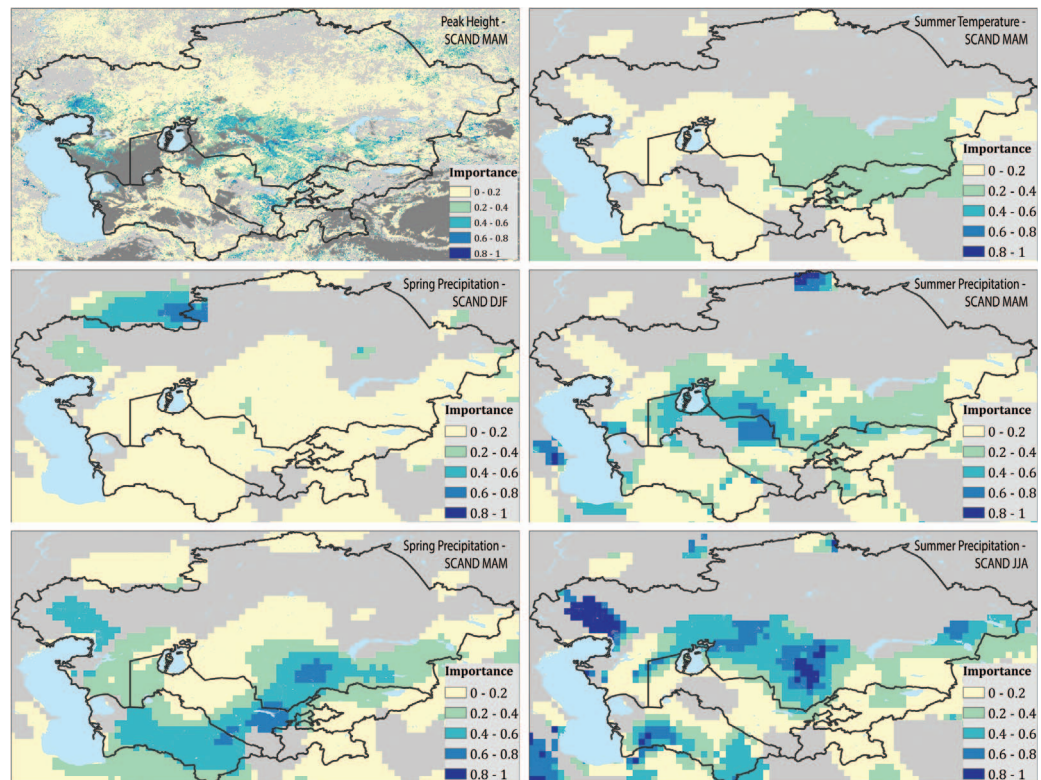


Figure 7. Impact of the SCAND index on the summer temperature, and spring and summer precipitation, as well as the peak height of the growing season. The peak height of the growing season reveals a significant impact in the southern third of Kazakhstan, co-located with the impact of spring SCAND on spring precipitation and summer and spring SCAND on summer precipitation.

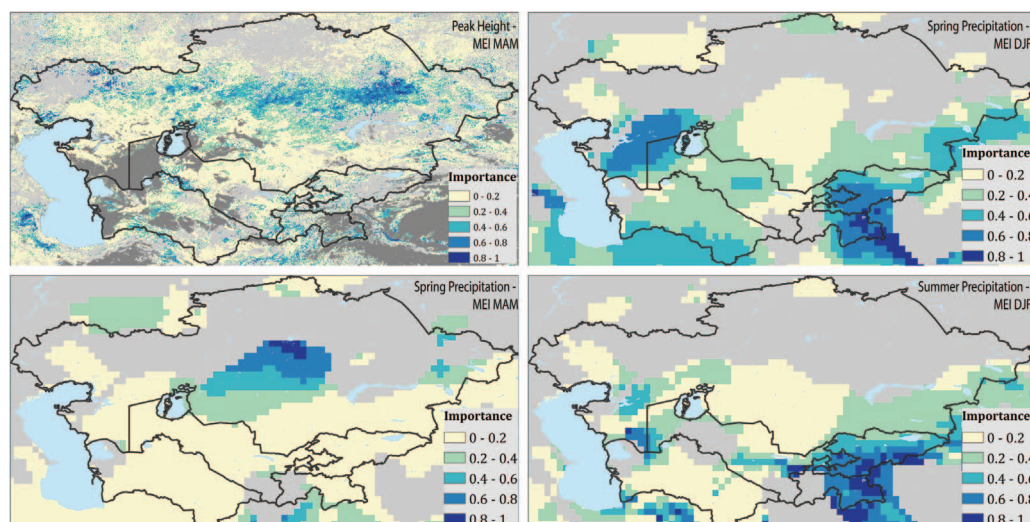


Figure 8. Winter MEI reveals strong importance on the spring and summer precipitation in Kyrgyzstan and Tajikistan with a subsequent effect on the land surface phenology in those countries as well. Spring MEI is very important for spring precipitation in central Kazakhstan, which is also reflected in the peak height results. Summer precipitation over montane Central Asia is linked to winter MEI.

Summer precipitation over montane Central Asia is linked to winter MEI (figure 8), which may be particularly relevant to regional hydrological assessments (Chen *et al* 2017, Chevallier *et al* 2014).

Thus, we find that while each of these indices has been mentioned in the literature as having an important impact on the weather of Central Asia, their impacts are often not co-located. Instead, NAO, EAWR, and AMO predominantly influence temperature in the northern part of Central Asia. When analyzed simultaneously, it is clear that NAO and EAWR reveal a more dominant impact on the weather and, subsequently, on the land surface phenology than AMO, which has a much slower tempo. While NAO has a strong influence in the northeastern part of the study region, EAWR influences the northwestern part. This pattern is an interesting result, especially considering that these two indices reveal a significant positive correlation. SCAND and MEI are not significantly correlated, but both reveal a significant impact on the precipitation in this region. Again, these impacts are not spatially co-located, with the MEI impacting the land surface phenology in the central part of the study region and SCAND having a greater effect slightly farther south.

Conclusions

Central Asia has been changing in multiple ways over the past few decades (de Beurs *et al* 2015, Groisman *et al* 2017). While human influences play a significant role in large swaths of Central Asia (e.g. de Beurs *et al* 2015, de Beurs and Henebry 2004, Kariyeva and van Leeuwen 2011, Kariyeva and van Leeuwen 2012, Lioubimtseva *et al* 2015, Lioubimtseva *et al* 2005), in this paper we have focused our attention on the effect of multiple climate oscillations on the weather

and land surface phenology of the region. Others have focused on the discrimination between weather changes and human impacts (e.g. Kariyeva *et al* 2012, Dubovyk *et al* 2016), but those studies did not identify the effect of large scale climate oscillations and regional climate patterns. Combining five climate oscillation indices into one regression model and then identifying the relative importance of each of these indices on precipitation and temperature and, subsequently, land surface phenology allowed us to identify where each of the climate indices displays its strongest influence. Our analysis demonstrates that the land surface phenology across Central Asia is affected by several climate modes, both those that are strongly linked to far northern weather patterns and those that are forced by southern weather patterns, making this region a ‘climate change hotspot’ (Bothe *et al* 2012) with strong spatial variations in weather patterns. We found that SCAND and EAWR, both regional climate patterns, played a significant role in Central Asia indicating that global climate patterns might not be sufficient to predict weather patterns and subsequent land surface changes in these regions (Chen *et al* 2016). These findings may also explain, in part, why both the CMIP3 and CMIP5 model cohorts exhibited large inter-model spread in montane Central Asia and why the CMIP5 models did not significantly improve precipitation estimates in this sensitive region (Flato *et al* 2013). Climate projections over mountainous terrain remain difficult (Flato *et al* 2013), particularly in Central Asia (Hijioka *et al* 2014, Reyser *et al* 2017).

Acknowledgments

This research was supported in part by the NASA Land Cover Land Use Change program through projects

NNX14AD88G, NNX14AJ32G, and NNX15AP81G. We thank Paul de Beurs for his software development that allowed us to run the land surface phenology analysis efficiently.

ORCID iDs

Kirsten M de Beurs  <https://orcid.org/0000-0002-9244-3292>

Geoffrey M Henebry  <https://orcid.org/0000-0002-8999-2709>

References

- Barlow M, Cullen H and Lyon B 2002 Drought in central and southwest Asia: La Nina, the warm pool, and Indian Ocean precipitation *J. Clim.* **15** 697–700
- Barlow M, Zaitchik B, Paz S, Black E, Evans J and Hoell A 2016 A review of drought in the Middle East and southwest Asia *J. Clim.* **29** 8547–74
- Barnston A G and Livezey R E 1987 Classification, seasonality and persistence of low-frequency atmospheric circulation patterns *Mon. Weather Rev.* **115** 1083–126
- Barriopedro D, Fischer E M, Luterbacher J, Trigo R M and García-Herrera R 2011 The hot summer of 2010: redrawing the temperature record map of Europe *Science* **332** 220–4
- Bocinsky R K and Kohler T A 2014 A 2, 000 year reconstruction of the rain-fed maize agricultural niche in the US Southwest *Nat. Commun.* **5** 5618
- Bothe O, Fraedrich K and Zhu X 2012 Precipitation climate of Central Asia and the large-scale atmospheric circulation *Theor. Appl. Climatol.* **108** 345–54
- Brunetti M and Kutiel H 2011 The relevance of the North-Sea Caspian Pattern (NCP) in explaining temperature variability in Europe and the Mediterranean *Nat. Hazards Earth Syst. Sci.* **11** 2881
- Chen Y, Li Z, Fang G and Deng H 2017 Impact of climate change on water resources in the Tianshan Mountains *Central Asia. Acta Geogr. Sin.* **72** 18–26
- Chen Y, Morton D C, Andela N, Giglio L and Randerson J T 2016 How much global burned area can be forecast on seasonal time scales using sea surface temperatures? *Environ. Res. Lett.* **11** 045001
- Chevallier P, Pouyaud B, Mojaiksky M, Bolgov M, Olsson O, Bauer M and Froebrich J 2014 River flow regime and snow cover of the Pamir Alay (Central Asia) in a changing climate *Hydrol. Sci. J.* **59** 1491–506
- Climate Prediction Center 2018 *Northern Hemisphere Teleconnection Patterns* (www.cpc.ncep.noaa.gov/data/teledoc/telecontents.shtml)
- de Beurs K M and Henebry G M 2004 Land surface phenology, climatic variation, and institutional change: analyzing agricultural land cover change in Kazakhstan *Remote Sens. Environ.* **89** 497–509
- de Beurs K M and Henebry G M 2005 Land surface phenology and temperature variation in the International geosphere–biosphere program high-latitude transects *Glob. Change Biol.* **11** 779–90
- de Beurs K M and Henebry G M 2008 Northern annular mode effects on the land surface phenologies of Northern Eurasia *J. Clim.* **21** 4257–79
- de Beurs K M and Henebry G M 2010 A land surface phenology assessment of the northern polar regions using MODIS reflectance time series *Can. J. Remote Sens.* **36** S87–110
- de Beurs K M, Henebry G M, Owsley B C and Sokolik I 2015 Using multiple remote sensing perspectives to identify and attribute land surface dynamics in Central Asia 2001–2013 *Remote Sens. Environ.* **170** 48–61
- de Beurs K M and Ioffe G 2014 Use of Landsat and MODIS data to remotely estimate Russia's sown area *J. Land Use Sci.* **9** 377–401
- Deser C, Knutti R, Solomon S and Phillips A S 2012 Communication of the role of natural variability in future North American climate *Nat. Clim. Change* **2** 775–9
- Dobson J E, Bright E A, Coleman P R, Durfee R C and Worley B A 2000 LandScan: a global population database for estimating populations at risk *Photogram. Eng. Remote Sens.* **66** 849–57
- Dubovyk O, Landmann T, Dietz A and Menz G 2016 Quantifying the impacts of environmental factors on vegetation dynamics over climatic and management gradients of central Asia *Remote Sens.* **8** 600
- Earth System Research Laboratory 2018a *AMO (Atlantic Multidecadal Oscillation) Index* (www.esrl.noaa.gov/psd/data/timeseries/AMO/)
- Earth System Research Laboratory 2018b *Multivariate ENSO Index (MEI)* (www.esrl.noaa.gov/psd/ens/mei/)
- Flato G *et al* 2013 Evaluation of climate models *Climate Change 2013: The Physical Science Basis. Contribution of Working Group I to the Fifth Assessment Report of the Intergovernmental Panel on Climate Change Climate Change 2013* ed T F Stocker vol 5 (Cambridge: Cambridge University Press) pp 741–866
- Groisman P *et al* 2017 Northern Eurasia Future Initiative (NEFI): facing the challenges and pathways of global change in the twenty-first century *Prog. Earth Planet. Sci.* **4** 41
- Harris I and Jones P D 2017 *CRU TS4.01: Climatic Research Unit (CRU) Time-Series (TS) version 4.01 of high resolution gridded data of month-by-month variation in climate (January 1901–December 2016)* (University of East Anglia Climatic Research Unit)
- Harris I, Jones P D, Osborn T J and Lister D H 2014 Updated high-resolution grids of monthly climatic observations—the CRU TS3.10 Dataset *Int. J. Climatol.* **34** 623–42
- Henebry G M and de Beurs K M 2013 Remote sensing of land surface phenology: a prospectus *Phenology: An Integrative Environmental Science* (Berlin: Springer)
- Hijioka Y, Lin E, Pereira J, Corlett R, Cui X, Insarov G, Lasco R, Lindgren E and Surjan A 2014 *Climate Change 2014: Impacts, Adaptation, and Vulnerability Part B: Regional Aspects. Contribution of Working Group II to the Fifth Assessment Report of the Intergovernmental Panel on Climate Change* ed V R Barros *et al* (Cambridge: Cambridge University Press) pp 1327–70
- Hu Z, Hu Q, Zhang C, Chen X and Li Q 2016 Evaluation of reanalysis, spatially interpolated and satellite remotely sensed precipitation data sets in central Asia *J. Geophys. Res. Atmos.* **121** 5648–63
- Hurrell J W 1995 Decadal trends in the North Atlantic Oscillation: regional temperatures and precipitation *Science* **269** 676–8
- Kariyeva J and van Leeuwen W J 2011 Environmental drivers of NDVI-based vegetation phenology in Central Asia *Remote Sens.* **3** 203–46
- Kariyeva J and van Leeuwen W J 2012 Phenological dynamics of irrigated and natural drylands in Central Asia before and after the USSR collapse *Agric. Ecosyst. Environ.* **162** 77–89
- Kariyeva J, van Leeuwen W J and Woodhouse C A 2012 Impacts of climate gradients on the vegetation phenology of major land use types in Central Asia 1981–2008 *Front. Earth Sci.* **6** 206–25
- Kazmin A S and Zatsepin A G 2007 Long-term variability of surface temperature in the Black Sea, and its connection with the large-scale atmospheric forcing *J. Marine Syst.* **68** 293–301
- Krichak S, Kishcha P and Alpert P 2002 Decadal trends of main Eurasian oscillations and the Eastern Mediterranean precipitation *Theor. Appl. Climatol.* **72** 209–20
- Kutiel H and Benaroch Y 2002 North Sea-Caspian Pattern (NCP)—an upper level atmospheric teleconnection affecting the Eastern Mediterranean: Identification and definition *Theor. Appl. Climatol.* **71** 17–28
- Lau W K and Kim K-M 2012 The 2010 Pakistan flood and Russian heat wave: Teleconnection of hydrometeorological extremes *J. Hydrometeorol.* **13** 392–403

- Lehmann E L and D'Abrera H 1998 *Nonparametrics: Statistical Methods Based on Ranks* vol 292 (Englewood Cliffs, NJ: Prentice-Hall) p 23
- Li J, Fan K and Xu Z 2016 Links between the late wintertime North Atlantic Oscillation and springtime vegetation growth over Eurasia *Clim. Dyn.* **46** 987–1000
- Li S, Perlwitz J, Quan X and Hoerling M P 2008 Modelling the influence of North Atlantic multidecadal warmth on the Indian summer rainfall *Geophys. Res. Lett.* **35**
- Lioubimtseva E 2015 A multi-scale assessment of human vulnerability to climate change in the Aral Sea Basin *Environ. Earth Sci.* **73** 719–29
- Lioubimtseva E, Cole R, ADAMS J M and Kapustin G 2005 Impacts of climate and land-cover changes in arid lands of Central Asia *J. Arid Environ.* **62** 285–308
- Lioubimtseva E, de Beurs K M and Henebry G M 2013 Grain production trends in the Russian Federation, Ukraine, and Kazakhstan in the context of the global climate variability and change *Climate Change and Water Resources* ed T Younos and C A Grady (Heidelberg: Springer)
- Lioubimtseva E, Dronin N M and Kirilenko A 2015 Grain production trends in the Russian Federation, Ukraine and Kazakhstan in the context of climate change and international trade *Climate Change and Food Systems: Global Assessments and Implications for Food Security and Trade* ed A Elbehri (Rome: Food Agriculture Organization of the United Nations)
- Lioubimtseva E and Henebry G M 2009 Climate and environmental change in arid Central Asia: Impacts, vulnerability, and adaptations *J. Arid Environ.* **73** 963–77
- Liu Y, Sun Q, Wang Z, Schaaf C and Erb A 2016 Evaluation of VIIRS daily BRDF, Albedo, and NBAR product using the MODIS Collection V006 product and *in situ* measurements *Geoscience and Remote Sensing Symposium (IGARSS), 2016 IEEE International (IEEE)* pp 1962–5
- Lyapustin A, Wang Y, Xiong X, Meister G, Platnick S, Levy R, Franz B, Korkin S, Hilker T and Tucker J 2014 Scientific impact of MODIS C5 calibration degradation and C6+ improvements *Atmos. Meas. Tech.* **7** 4353–65
- Oguz T, Dippner J W and Kaymaz Z 2006 Climatic regulation of the Black Sea hydro-meteorological and ecological properties at interannual-to-decadal time scales *J. Marine Syst.* **60** 235–54
- Reyer C P, Otto I M, Adams S, Albrecht T, Baarsch F, Carlsburg M, Coumou D, Eden A, Ludi E and Marcus R 2017 Climate change impacts in Central Asia and their implications for development *Reg. Environ. Change* **17** 1639–50
- Schaaf C B *et al* 2002 First operational BRDF, albedo nadir reflectance products from MODIS *Remote Sens. Environ.* **83** 135–48
- Schlesinger M E and Ramankutty N 1994 An oscillation in the global climate system of period 65–70 years *Nature* **367** 723
- Sommer R, Glazirina M, Yuldashev T, Otarov A, Ibraeva M, Martynova L, Bekenov M, Kholov B, Ibragimov N and Kobilov R 2013 Impact of climate change on wheat productivity in Central Asia *Agric. Ecosyst. Environ.* **178** 78–99
- Stöckli R and Vidale P L 2004 European plant phenology and climate as seen in a 20 year AVHRR land-surface parameter dataset *Int. J. Remote Sens.* **25** 3303–30
- Syed F, Giorgi F, Pal J and King M 2006 Effect of remote forcings on the winter precipitation of central southwest Asia part 1: observations *Theor. Appl. Climatol.* **86** 147–60
- Tüshaus J, Dubovyk O, Khamzina A and Menz G 2014 Comparison of Medium Spatial Resolution ENVISAT-MERIS and Terra-MODIS time series for vegetation decline analysis: a case study in Central Asia *Remote Sens.* **6** 5238–56
- Wang D, Morton D, Masek J, Wu A, Nagol J, Xiong X, Levy R, Vermote E and Wolfe R 2012 Impact of sensor degradation on the MODIS NDVI time series *Remote Sens. Environ.* **119** 55–61
- Wolter K and Timlin M S 1998 Measuring the strength of ENSO events: how does 1997/98 rank? *Weather* **53** 315–24
- Wright C K, de Beurs K M and Henebry G M 2014 Land surface anomalies preceding the 2010 Russian heat wave and a link to the North Atlantic oscillation *Environ. Res. Lett.* **9** 124015
- Zheng Z and Zhu W 2017 Uncertainty of Remote Sensing Data in Monitoring Vegetation Phenology: A Comparison of MODIS C5 and C6 Vegetation Index Products on the Tibetan Plateau *Remote Sens.* **9** 1288
- Zuber V and Strimmer K 2011 High-dimensional regression and variable selection using CAR scores *Stat. Appl. Genet. Mol. Biol.* **10** 1544–6115